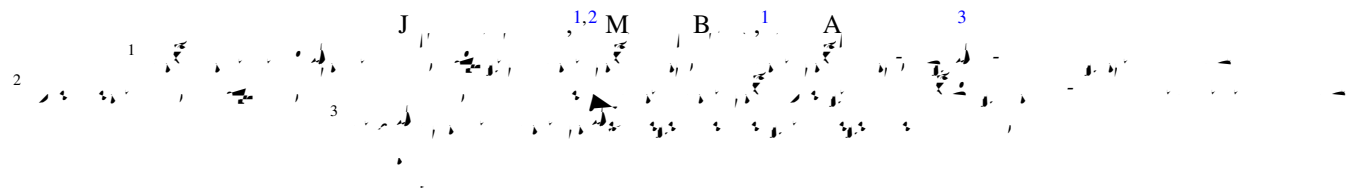
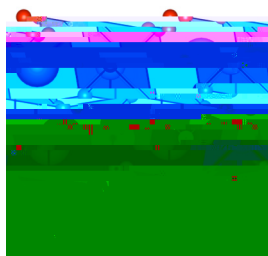


O  $\rightarrow$   $\mathbf{e}_1$   $\mathbf{e}_2$   $\mathbf{e}_3$   $\mathbf{e}_4$   $\mathbf{e}_5$   $\mathbf{e}_6$   $\mathbf{e}_7$   $\mathbf{e}_8$   $\mathbf{e}_9$   $\mathbf{e}_{10}$   $\mathbf{e}_{11}$   $\mathbf{e}_{12}$   $\mathbf{e}_{13}$   $\mathbf{e}_{14}$   $\mathbf{e}_{15}$   $\mathbf{e}_{16}$   $\mathbf{e}_{17}$   $\mathbf{e}_{18}$   $\mathbf{e}_{19}$   $\mathbf{e}_{20}$   $\mathbf{e}_{21}$   $\mathbf{e}_{22}$   $\mathbf{e}_{23}$   $\mathbf{e}_{24}$   $\mathbf{e}_{25}$   $\mathbf{e}_{26}$   $\mathbf{e}_{27}$   $\mathbf{e}_{28}$   $\mathbf{e}_{29}$   $\mathbf{e}_{30}$   $\mathbf{e}_{31}$   $\mathbf{e}_{32}$   $\mathbf{e}_{33}$   $\mathbf{e}_{34}$   $\mathbf{e}_{35}$   $\mathbf{e}_{36}$   $\mathbf{e}_{37}$   $\mathbf{e}_{38}$   $\mathbf{e}_{39}$   $\mathbf{e}_{40}$   $\mathbf{e}_{41}$   $\mathbf{e}_{42}$   $\mathbf{e}_{43}$   $\mathbf{e}_{44}$   $\mathbf{e}_{45}$   $\mathbf{e}_{46}$   $\mathbf{e}_{47}$   $\mathbf{e}_{48}$   $\mathbf{e}_{49}$   $\mathbf{e}_{50}$   $\mathbf{e}_{51}$   $\mathbf{e}_{52}$   $\mathbf{e}_{53}$   $\mathbf{e}_{54}$   $\mathbf{e}_{55}$   $\mathbf{e}_{56}$   $\mathbf{e}_{57}$   $\mathbf{e}_{58}$   $\mathbf{e}_{59}$   $\mathbf{e}_{60}$   $\mathbf{e}_{61}$   $\mathbf{e}_{62}$   $\mathbf{e}_{63}$   $\mathbf{e}_{64}$   $\mathbf{e}_{65}$   $\mathbf{e}_{66}$   $\mathbf{e}_{67}$   $\mathbf{e}_{68}$   $\mathbf{e}_{69}$   $\mathbf{e}_{70}$   $\mathbf{e}_{71}$   $\mathbf{e}_{72}$   $\mathbf{e}_{73}$   $\mathbf{e}_{74}$   $\mathbf{e}_{75}$   $\mathbf{e}_{76}$   $\mathbf{e}_{77}$   $\mathbf{e}_{78}$   $\mathbf{e}_{79}$   $\mathbf{e}_{80}$   $\mathbf{e}_{81}$   $\mathbf{e}_{82}$   $\mathbf{e}_{83}$   $\mathbf{e}_{84}$   $\mathbf{e}_{85}$   $\mathbf{e}_{86}$   $\mathbf{e}_{87}$   $\mathbf{e}_{88}$   $\mathbf{e}_{89}$   $\mathbf{e}_{90}$   $\mathbf{e}_{91}$   $\mathbf{e}_{92}$   $\mathbf{e}_{93}$   $\mathbf{e}_{94}$   $\mathbf{e}_{95}$   $\mathbf{e}_{96}$   $\mathbf{e}_{97}$   $\mathbf{e}_{98}$   $\mathbf{e}_{99}$   $\mathbf{e}_{100}$





Q



$\mathcal{H} = \mathcal{H}_0 + \mathcal{H}_1$  with  $\mathcal{H}_0 = \sum_{i=1}^3 \frac{p_i^2}{2m_i} + \sum_{i=1}^3 \frac{1}{2} m_i \omega_i^2 x_i^2$  and  $\mathcal{H}_1 = \sum_{i=1}^3 \lambda_i x_i^3$  ( $\lambda_i = 0, F$ )  
 with  $\mathcal{H}_0$  and  $\mathcal{H}_1$  being the unperturbed and the perturbation Hamiltonian, respectively.

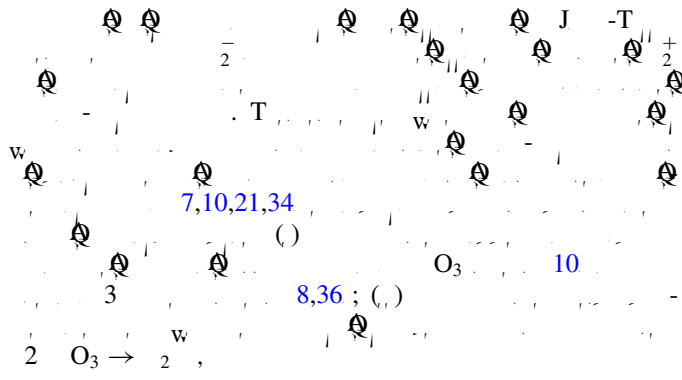


TABLE I. DFT results for the energy splitting of the  $E_g$  bands in the pnictides.

$E_g$	Symmetry	$(\sqrt{2}, \sqrt{2}, 2)$ (GGA + $U$ )		$P_4$ (HSE06)	
		$\Delta_{OBS}$	OBS (meV)	$\Delta_{OBS}$	OBS (meV)
$L T_2 O_3$	$1 (2 \uparrow)$	0	(0)	0	0
$L M O_3$	$4 (2 \uparrow, 2 \downarrow)$	0	(0)	0	0
$L O_3$	$2 (2 \uparrow)$	-297	(-237)	0.42	-428
$KF F_3$	$6 (2 \uparrow, 2 \downarrow, 2 \uparrow, 2 \downarrow)$	-	-	-	-

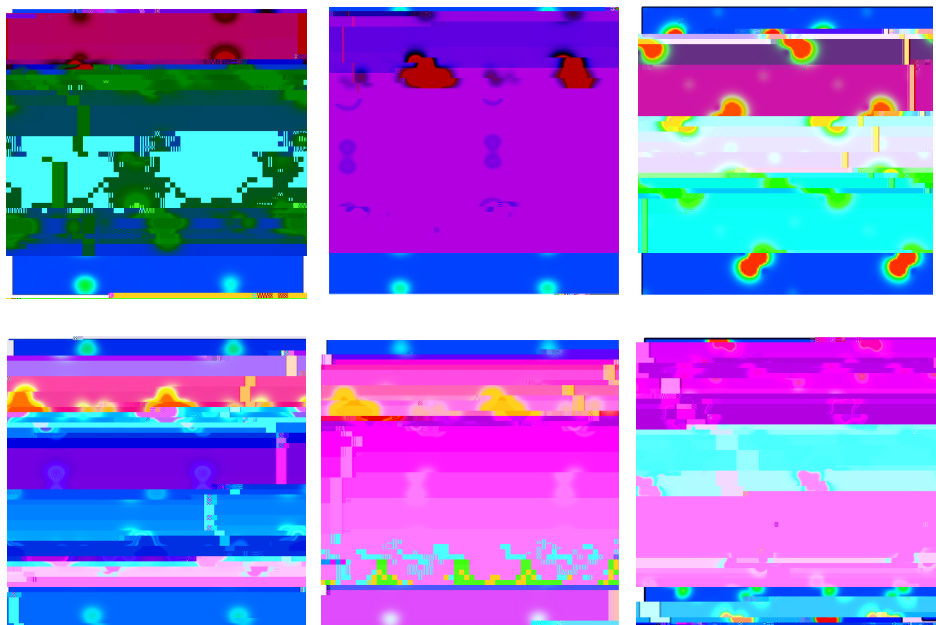




TABLE II. A summary of the ground state configurations and the corresponding magnetic moments for the  $Q_2^+$  phase of  $\text{LaT}_x\text{O}_3$  and  $\text{LaM}_x\text{O}_3$  for various values of  $x$ . The magnetic moments are given in  $\mu_B$ . The ground state configurations are labeled by their symmetry: AFMG (antiferromagnetic G-type), AFMA (antiferromagnetic A-type), and AFMC (antiferromagnetic C-type). The magnetic moments are given in  $\mu_B$ . The ground state configurations are labeled by their symmetry: AFMG (antiferromagnetic G-type), AFMA (antiferromagnetic A-type), and AFMC (antiferromagnetic C-type).

	$Q_2^+$	M	$Q_2^+$	S	$\frac{1}{2}(\frac{1}{3})C_1(Q_2^+)$ (E <sub>g</sub> )	$\frac{1}{2}(\frac{2}{3})C_2(Q_2^+)$ (E <sub>g</sub> )
L T <sub>0.93</sub> O <sub>3</sub>	0.93	AFMG		$\frac{1}{2}$	0.040 (0.041 56)	
L M <sub>0.94</sub> O <sub>3</sub>	0.94	AFMA		1	0.324 (0.357 30)	
L <sub>0.95</sub> O <sub>3</sub>	0.95	AFMC		$\frac{2}{3}$	0.005 (0.009 57)	0.093 (0.079 57)
KF F <sub>3</sub>	1.00	AFMG		$\frac{1}{2}$	0.078 (0.090 58)	0.104 ( )
KC F <sub>3</sub>	1.01	AFMG		1		0.003 ( )
KC F <sub>3</sub>	0.99	AFMA		$\frac{2}{3}$		0.336 (0.316 28)
KC F <sub>3</sub>	1.03	AFMA		$\frac{4}{3}$		0.300 (0.299 28)
KC F <sub>3</sub>	1.03	AFMA		$\frac{4}{3}$		0.335 (0.355 29)

C. T<sub>0.93</sub>O<sub>3</sub> and LaM<sub>0.94</sub>O<sub>3</sub> as a function of  $x$ .



F. 4, DMFT (F. 8 R. 3),

J-T, C, AFM,  $(\sqrt{2}, \sqrt{2}, 2)$ ,  $O_{3w}$ , S III A), AFM,  $(\Delta_{\phi} = -74)$ , AFM,  $(\Delta_{\phi} = -34)$ , T,  $O_3$ , T, I, R, 21, T,  $(\sqrt{2}, \sqrt{2}, 2)$ ,  $O_3$ .

2. The origin of the improper  $Q_2^+$  motion in LaMnO<sub>3</sub>

O, A, LM O<sub>3</sub>, C, 30, 64, T, LM O<sub>3</sub>, J, -T, LM O<sub>3</sub>, O, LM O<sub>3</sub>, 750 K, R, 30, U, A, G, T.

3. The origin of the orbital ordering in RTMnO<sub>3</sub> (R = La, Y)

A, LM O<sub>3</sub>, LT O<sub>3</sub>, J, -T, J, R, 34, LM O<sub>3</sub>, T,  $\alpha, \beta, \gamma$ ,  $\alpha, \beta, \gamma$ , R, 34.

D. C. e. Ja. Te. e. effec. a. d. e. ca.  $2^2$ . d. ced.  $Q_2^+$ . de. a. ec. e. f. ee. a. ed. - b. a. e. e.  $RVO_3$ . c. d.

A, T, LM O<sub>3</sub>, J, -T, O<sub>3</sub> (= L-L), O, LM O<sub>3</sub>, 6, C, 21, 55, O<sub>3</sub>, 0 K, I.

AFMG AFMC : ( )  $\frac{+}{2}$   
w w ( )  $\frac{-}{2}$   
T  $\frac{+}{2}$  S III C  
10 J -T A H)  
O w 31,55  
 $\frac{-}{2}$   $\frac{+}{2}$  J -T

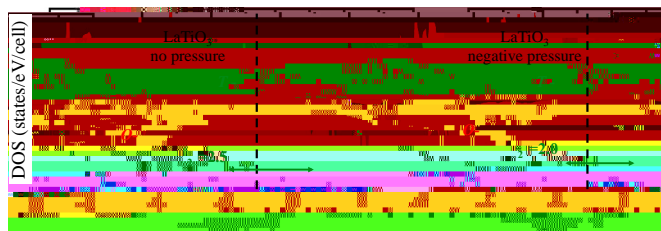


FIG. 6. Pressure dependence of the density of states (DOS) for  $\text{LaTiO}_3$ . The DOS is shown for the no pressure (left) and negative pressure (right) cases. The Fermi level is indicated by a dashed horizontal line.

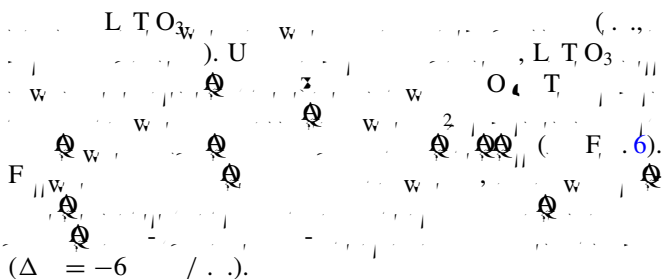
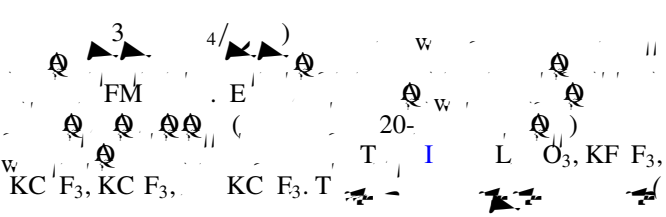
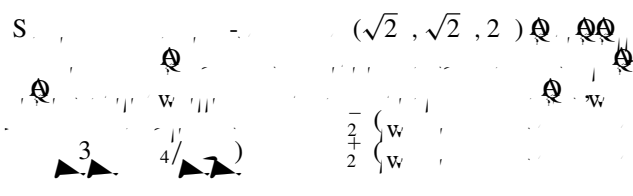


TABLE I. Energy levels  $E_i$  (in eV) for the  $t_{2g}$  and  $e_g$  states. The values are given for the FM state. The energy is measured relative to the Fermi level.

State	$\Delta_{2+} (eV)$	$\Delta_{2-} (eV)$
$KF F_3$	-2739	-2760
$KC F_3$	-2976	-3004
$L O_3$	-1153	-1325
$KC F_3$	-1295	-1298
$KC F_3$	-1019	-1020



APPENDIX C: ENERGY GAIN ASSOCIATED WITH  $Q_2^+$  AND  $Q_2^-$  OCTAHEDRAL DEFORMATION MODE





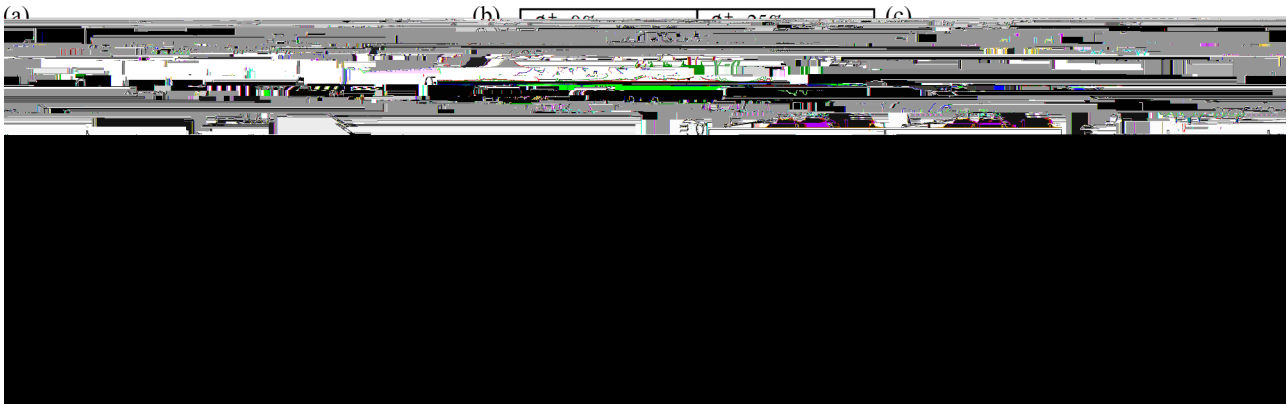
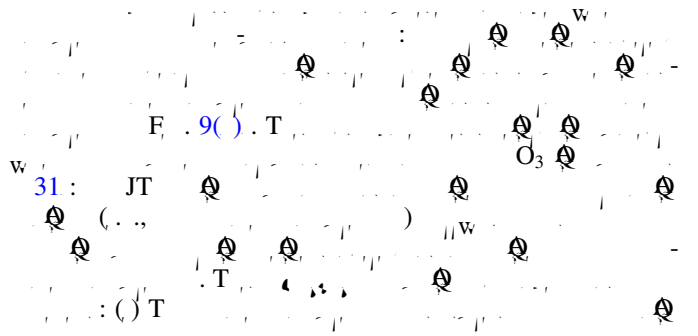
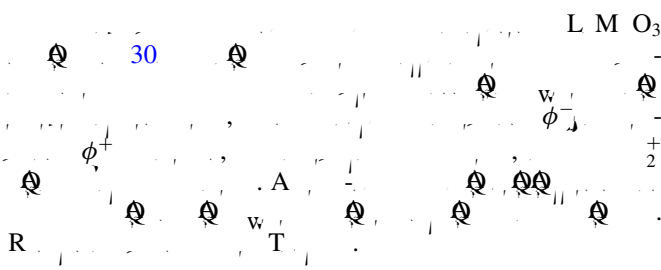
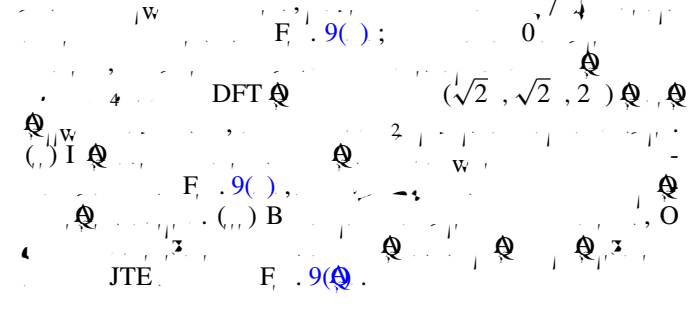
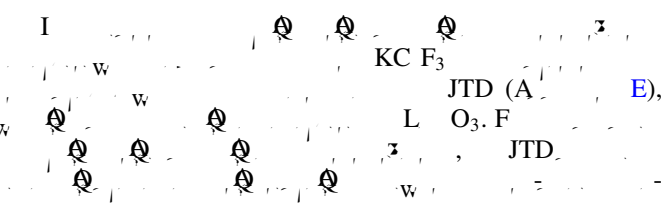


FIG. 9. Crystal structure and magnetic ordering of  $\text{LaMnO}_3$ . (a) Crystal structure showing Mn (red), O (green), and La (blue) ions. (b) Magnetic structure showing Mn<sup>3+</sup> (red) and Mn<sup>4+</sup> (green) ions with their spin orientations. (c) Crystal structure showing Mn (red), O (green), and La (blue) ions with the Jahn-Teller distortion (JTD) indicated by the displacement of Mn ions.

APPENDIX G: SYMMETRY MODE ANALYSIS OF  $\text{LaMnO}_3$  EXPERIMENTAL STRUCTURES



APPENDIX H: COOPERATING AND COMPETING OCTAHEDRAL ROTATIONS AND JAHN-TELLER EFFECT IN  $\text{LaVO}_3$



1 H. B. (S), B. H. K., D. R. (2009).  
 2 D. I. K. (C) - T

- 8 G. T. [Q.](#), [J. A.](#), [P. R. B](#) **97**, 035107 (2018).
- 9 G. M. D. [J.](#), Q. L. [J.](#), M. B. [J.](#), A. [J.](#), [P. R. B](#) **98**, 075135